Proteomic analysis reveals potential biomarker candidates in serous ovarian tumors – a preliminary study

Shona Pedersen[1], Alaaeldin Ali Mohamed[1], Hubert Krzyslak[2], Latifa Saad S A Al-Kaabi[1], Mohannad Natheef Abuhaweeleh[1], Ala-Eddin Al Moustafa[1], Lina Ghabreau[3], Semir Vranic[1], Bent Honoré[4]

[1]College of Medicine, QU Health, Qatar University, Doha, Qatar
[2]Department of Clinical Biochemistry, Aalborg University Hospital, Aalborg, Denmark
[3]Faculty of Medicine, University of Aleppo, Aleppo, Syria
[4]Department of Biomedicine, Aarhus University, Aarhus, Denmark

Introduction: Ovarian serous cystadenocarcinoma (SCA), a deadly gynecologic cancer, often goes undetected until the late stages. Tissue proteomics unveils disease heterogeneity, enhancing tumor classification and enabling personalized treatments tailored to individual expression profiles.

Material and methods: Tissue samples from 46 serous ovarian tumors were quantified using label-free liquid chromatography-tandem mass spectrometry. We identified 80 proteins differentiating SCA from borderline tumors, 277 distinguishing SCA from benign tumors, and 195 between borderline and benign tumors. Ingenuity pathway analysis revealed increased cell proliferation and RNA processing in SCA and borderline tumors compared to benign tumors, with SCA showing greater oxidative phosphorylation than borderline tumors.

Results: Our comparative analysis indicates that upregulated (ASS1 – argininosuccinate synthase 1, CAPS, PPA1, BCAT1, MCM4) and downregulated proteins (MUC5B, SLC4A1, tenascin-XB – TNXB, carbonic anhydrase 1, hemoglobin β) may offer a robust panel for distinguishing SCA from benign and borderline ovarian tumors, potentially aiding in early diagnosis and disease monitoring. The cancer-associated proteins pyridoxal dependent decarboxylase domain containing 1 (AUC: 0.83, 95% CI: 0.66–1), GFPT1 (AUC: 0.84, CI: 0.70–0.89), and HYOU1 (AUC: 0.84, CI: 0.70–0.98) significantly differentiated between low-grade (LGSCA) and high-grade serous cystadenocarcinoma (HGSCA). Low-grade SCA showed significantly greater levels of MZB1 ($\log_2$ fold change (FC): –1.951, *p*-value: 0.0258), CRABP2 (FC: –2.34, *p*-value: 0.0016), and BCAM (FC: –1.945, *p*-value: 0.0197) than borderline cancers.

Conclusions: Argininosuccinate synthase 1 and TNXB showed potential as markers of disease progression. Elevated ASS1 was observed in borderline, LGSCA, and HGSCA tumors compared to benign tumors, while TNXB levels progressively declined from benign to borderline, LGSCA, and HGSCA tumors. Our study pinpoints critical biomarkers in serous ovarian tumors for HGSCA progression.

Key words: ovarian cancer, formalin-fixed paraffin-embedded tissue, protein biomarkers, mass spectrometry, proteomics.

Contemp Oncol (Pozn) 2025; 29 (1): 77–92
DOI: https://doi.org/10.5114/wo.2025.149180

Introduction

Ovarian cancer has the worst prognosis and the highest mortality rate of any gynecological cancer [1–4]. This is primarily because most patients have advanced serous ovarian carcinomas, which frequently develop resistance to platinum/taxane chemotherapy [4, 5]. Malignant ovarian tumors comprise three cell types: epithelial, stromal, and germ cells [6, 7]. Epithelial tumors (carcinomas) account for 90% of all ovarian cancers, which are further classified into two types based on biological characteristics and clinical behavior: low-grade serous ovarian cystadenocarcinoma (LGSCA) and high-grade serous ovarian cystadenocarcinoma (HGSCA) [8–10]. Serous borderline tumors represent non-invasive, low-grade, proliferative serous epithelial neoplasms falling between benign cystadenomas and serous cystadenocarcinoma (SCA) [11]. A subset of borderline ovarian tumors are precursors of LGSCA [12, 13].

Currently, the standard method for diagnosing a suspected lesion is a surgical exploration to obtain a tissue sample, followed by histological confirmation. Despite its high specificity, a meta-analysis suggests that the frozen section has low sensitivity for borderline tumors, mucinous tumors, and larger neoplasms [14]. In addition to differences in biomarker concentrations between formalin-fixed paraffin-embedded (FFPE) tissue specimens and plasma, tumor heterogeneity may limit the diagnostic value of plasma proteins [15].

Several studies have suggested that inherited or sporadic mutations in the *BRCA1* and *BRCA2* genes may increase the risk of ovarian cancer [16, 17]. The most prevalent subtype of type II tumors, HGSCA, is associated with relative chromosomal instability and mutations in the *TP53* (96%) and *BRCA1* (22%) genes [16–20]. However, it is believed that BRCA1 mutations cannot accurately predict disease progression without additional biomarkers but may predict response to the targeted treatment with poly-ADP ribose polymerase inhibitors. Protein biomarkers have been proposed as a promising tool for diagnosis and treatment, but their effectiveness is yet to be established.

However, specific biomarkers, such as cancer antigen 125 (CA125) and human epididymis protein 4 (HE4) [21–25], have been validated and are currently used to monitor treatment and identify recurrence in ovarian cancer patients. Despite the prevalence of serum CA125 measurement and ultrasonography [26] in ovarian cancer diagnosis, their early detection accuracy is limited due to false positive and false negative results. *In vitro* multivariate index assays (IVDMIAs) that include multiple markers have been developed to improve the diagnostic accuracy of ovarian cancer assessment [27, 28]. Before surgery, OVA1 was the first IVDMIA to assess the likelihood of malignancy in women

with an ovarian adnexal mass [28, 29]. ROMA is an additional biomarker assay that determines the risk of ovarian cancer by analyzing serum concentrations of CA125 and HE4 [25, 30, 31], in addition to menopausal status [32]. The Overa test, the successor to OVA1, replaces two biomarkers in OVA1 with HE4 and follicle-stimulating hormone and provides a malignancy probability score ranging 0–10 [27, 28]. In the early stages of ovarian cancer, the survival rate is high, but it drops significantly in later stages. Unfortunately, ovarian cancer symptoms typically do not manifest until later stages, highlighting the urgent need for a screening test and early detection method that can identify biomarker changes at an early stage.

Limitations in current testing methods hinder the accurate detection of early-stage ovarian tumors [33]. Hence, it is crucial to explore more sensitive diagnostic biomarkers and develop novel treatment strategies. Integrating targeted and untargeted proteomics with biostatistics holds promise in creating innovative tools to significantly reduce ovarian cancer mortality rates [34–37]. Proteomics, known for its high specificity and sensitivity in various cancers, including ovarian cancer [38–41], has been utilized through mass spectrometry-based approaches to comprehend the disease's pathology and identify specific biomarkers for early detection [35, 42]. Additionally, it aids in the identification of biomarkers associated with chemotherapy resistance [43, 44], a critical factor affecting treatment management and cancer progression. Personalized treatment based on these biomarkers can yield improved patient outcomes.

To contribute to this effort, we analyzed the proteomes of FFPE tissue biopsies obtained from different types of serous ovarian tumors, including benign tumors, borderline tumors, and SCA. Additionally, we investigated the proteins that showed abnormal regulation in HGSCA and LGSCA, as well as in borderline tumors compared to LGSCA. We aimed to discover markers of disease progression and assess the proteins specific to the tissue that are linked to the development of serous ovarian tumors.

Materials and methods

Study demographics and sample selection

Forty-six patients with serous ovarian tumors were selected for the current study (8 LGSCA, 26 HGSCA). All the patients were diagnosed and treated at the University of Aleppo Hospital. Two board-certified pathologists (L.G. and S.V.) reviewed all the cases, confirmed the diagnoses, and selected the samples for the current study. Only samples with > 80% vital tumor and available remaining tissue were selected for the study. Other subtypes of ovarian carcinomas (mucinous, clear cell, endometrioid), metastatic tumors, and non-epithelial tumors (germ cell, sex cord-stromal tumors) of the ovary were excluded from the study. Serous cystadenocarcinoma was graded using the two-tiered grading system: low-grade (well-differentiated) and high-grade (poorly differentiated) cancers. The tumor staging was done using the International Federation of Gynecology and Obstetrics (FIGO) system. Serum CA125 levels were routinely assessed in all patients during the diagnostic work-up and before surgery, by the local protocol in the hospital. None of the patients received chemo- or radiotherapy before the sampling.

Preparation of formalin-fixed paraffin-embedded tissue and analysis by LC-MS/MS

Forty-six FFPE samples comprising three benign, nine borderline, and 34 SCA were prepared for proteomic analysis. The paraffin was removed from seven slices of 10 µm with xylene, followed by rehydration with decreasing levels of ethanol/water, and then they were dried as previously described [45]. The tissue was then dissolved in lysis buffer (5% sodium dodecyl sulfate, 50 mM triethylammonium bicarbonate, pH 8.5), and the protein concentration was estimated using infrared spectrometry (Direct Detect Spectrometer, Merck KGaA, Darmstadt, Germany). Tryptic digestion was performed using S-Trap micro spin columns (Protifi, Farmingdale, Huntington, NY, USA), as previously described [46]. A set of samples was further purified using C18 spin columns. The peptide concentration was estimated by tryptophan fluorescence [45], and finally, samples were dissolved in 0.1% formic acid and 1 µg of each sample was injected in one to four replicates into a Dionex Ultimate 3000 RSCL nano-LC system (Thermo Fisher Scientific Instruments, Waltham, MA, USA). Samples were loaded and trapped on a µ-Precolumn (300 µm × 5 mm, C18 PepMap100, 5 µm, 100 Å (Thermo Fisher Scientific, Waltham, MA, USA) with a flow rate of 30 µl/min using 97.9% (vol/vol) water, 2% (vol/vol) acetonitrile and 0.1% (vol/vol) formic acid. Peptide separation was performed with a flow of 300 nl/min using an analytical column (EASY-Spray Column, 500 mm × 75 µm, PepMap RSCL, C18, 2 mm, 100 Å, Thermo Scientific). Peptides were eluted using a gradient by mixing buffer A (99.9% (vol/vol) water, 0.1% (vol/vol) formic acid) with buffer B (99.9% (vol/vol) acetonitrile, 0.1% (vol/vol) formic acid) over 181 min. The gradient was initiated with 2% B at 0 min, 14% B at 3 min, 25% B at 120 min, 40% B at 125 min, 80% B at 127 min, 80% B at 143 min and 2% B at 144 min to 181 min. The acquisition was performed on an Orbitrap Fusion Tribrid mass spectrometer (Thermo Scientific). The universal method setting was used with a duration of 152 min. Peptides with charge states of 2–7 were included. The cycle time was 3 s. Dynamic exclusion was set to 60 s. MS^1 was performed with full orbitrap scans (m/z 375–1500) at a resolution of 120,000 with an automatic gain control (AGC) target of 4×10^5 and a maximum injection time of 50 ms. The most intense precursors were selected with an intensity threshold of 5×10^3 to a maximum of 1×10^{20}. For MS^2 scans precursor ions were isolated in the quadrupole with an isolation window of 1.6 m/z. MS^2 scans were performed at a rapid scan rate in the linear ion trap with collision-induced dissociation energy at 35%, an AGC target of 2×10^3, and a maximum injection time of 300 ms, as previously described [46]. The MS analysis generated 184 raw files. The raw files were analyzed with MaxQuant version 1.6.5.0 (Max Planck Institute of Biochemistry, Martinsried, Germany) for label-free quantification (LFQ) analysis [47]. The database searched was Uniprot *Homo sapiens* (filtered and reviewed) (www.uniprot.org), downloaded on

10 August 2022. MaxQuant settings have previously been described [48]. In short, we generally used the default setting for LFQ analysis with a false discovery rate (FDR) of 0.01 for protein identification and peptide spectrum matches. Trypsin digestion was used instead of Trypsin/P. The label-free quantification minimum ratio count was set to 1. The "match between runs" function was activated. MS/MS was required for quantification. Peptides used for quantification were unique and razor peptides, unmodified and modified with oxidation (M) or acetyl (protein N-terminal). A Decoy search was performed in the database with revert sequences. The search included contaminant sequences. The MaxLFQ algorithm in MaxQuant performs a very robust "delayed normalization" procedure [49]. MaxQuant data can be found in Supplementary File 1.

Statistical analysis

Demographic and clinical data were examined using IBM SPSS Statistics 29.0.0.0 (IBM Corp., Armonk, NY, USA) and displayed as mean and standard deviations (mean ±SD). Age disparities among the study groups were explored using ANOVA (analysis of variance) with Games-Howell *post hoc* analysis. Within the SIMCA software, we conducted an unsupervised principal component analysis to evaluate trends and detect potential outliers in the dataset (Suppl. File 2, Fig. S1). To pinpoint proteins with significant contributions to group differentiation, we utilized OPLS-DA, a supervised multivariate analysis technique. Both principal component analysis and OPLS-DA analyses were carried out on proteomic data that had been transformed logarithmically. In Perseus versions 1.6.14.0 or 2.0.7.0 (Max Planck Institute of Biochemistry, Martinsried, Germany) [47], the LFQ data of the identified proteins extracted from the MS were $\log_2$ transformed, and technical replicate values were averaged to obtain a single value for each biological replicate. Data were further filtered by excluding potential contaminants, reverse sequences, and proteins only identified by site. For a successful identification, it was essential for a protein to possess at least 2 unique peptides. A protein needed to exhibit a minimum of 70% valid values within every group. For group comparison analysis, we applied a stringent statistical methodology. Depending on the specific nature of the comparisons, we either used parametric tests (such as Student's *t*-test and ANOVA coupled with Tukey's HSD *post hoc* test) or their non-parametric counterparts (such as the Mann-Whitney *U* test and Kruskal-Wallis *H* test, complemented by Bonferroni correction). Significance thresholds were set at $p < 0.05$ and a $\log_2$ fold change ($\log_2$FC) > 1 or < –1. In cases of multiple ANOVA testing, we adopted a permutation-based FDR technique, using 250 randomizations, and presented the findings as *q*-values.

The chosen models and biomarker candidates were visualized and presented in the form of individual receiver operating characteristic (ROC) curves. Statistical analysis was performed using GraphPad Prism 9.5.1 (GraphPad Software, La Jolla, CA, USA) and Microsoft Excel. To conduct PCA and OPLS-DA analyses, SIMCA 17 software (Sartorius, Göttingen, Germany) was used. For the combined ROC analysis metaboanalyst v. 6.0 was used (https://www.metaboanalyst.ca/home.xhtml). The relevant log transformed MS data for proteins were tested using the "ROC curve-based model evaluation" under Biomarker analysis. The chosen algorithm for both combined models is the random forest.

For the pathway analysis, data were analyzed with ingenuity pathway analysis (IPA) from QIAGEN Inc., (https://www.qiagenbioinformatics.com/products/ingenuity-pathway-analysis). The algorithms developed for use in IPA are described by Krämer *et al*. [50]. Of the 1,736 proteins uploaded 1,725 proteins were recognized by IPA. Analysis was performed on proteins that were significantly changed based on a *t*-test at $p < 0.05$ (Suppl. File 3).

Results

Clinicopathologic characteristics of the cohort

The clinicopathologic characteristics of the cohort are presented in Table 1. During the study period, 34 patients with SCA and 9 with borderline serous ovarian cystadenomas met the inclusion requirements and participated in the study. In addition, 3 benign serous cystadenomas were gathered as control samples. Over 90% of the SCA patients were identified with early-stage disease (FIGO stage I). Regarding tumor grade, more than 75% of the SCA patients presented with HGSCA (Table 1). As anticipated, age correlated significantly with the type of the disease.

Distinct tissue-enriched proteomic profile between benign tumors, borderline tumors, and serous cystadenocarcinoma

Using mass spectrometry, 3802 proteins were detected, with 1736 identified in at least 70% of samples within each group (Suppl. File 1). The unsupervised PCA identified three groups with some overlap between them (Suppl. File 2, Fig. S1). In addition, a multivariate analysis using orthogonal partial least squares discriminant analysis (OPLS-DA) was performed to include the integrated protein profiles found in SCA, borderline, and benign cases (Fig. 1 A). Interestingly, the participants in the study were found to cluster based on their respective groups, with two principal components (PC1 and PC2) accounting for 95% of the subject clustering (R2X = 0.490, Q2 = 0.245 (Comp1) (R2Y = 0.801, Q2 = 0.258) (Comp2). This suggests that the protein profiles of each group were unique and contributed to the observed discrimination. A heat map was also used to show the differences in protein abundance between the three groups (Fig. 1 B). Finally, volcano plots were used to demonstrate fold changes in protein expression between various group comparisons: SCA vs. borderline showed 53 upregulated and 27 downregulated proteins (Fig. 1 C, Suppl. File 1), SCA vs. benign revealed 255 upregulated and 22 downregulated proteins (Fig. 1 D, Suppl. File 1), and benign vs. borderline showed 175 upregulated and 20 downregulated proteins (Fig. 1 E, Suppl. File 1). Table 2 shows the pairwise comparison of the top 10 proteins with differential expression between SCA vs. borderline, SCA vs. benign, and borderline vs. benign, with $\log_2$FC > 1 or < –1. Supplementary File 1 provides additional information on all significantly expressed proteins.

Table 1. Patient and tumor characteristics of the ovarian cancer cohort

Parameters	Benign (*n* = 3)	Borderline (*n* = 9)	SCA (*n* = 34)	*p*-value*
	Mean ± SD	Mean ± SD	Mean ± SD	
Demographics				
Age (years)	29.3 ±1.5	37.6 ±11.9	48.9 ±12.0	0.004
Biochemical measurements				
CA125	–	+	≥ + +	–
FIGO staging of SCA				
Stage I, *n* (%)	–	–	31 (91.2)	
Stage II, *n* (%)	–	–	0 (0)	
Stage III, *n* (%)	–	–	3 (8.8)	
Grading of SCA				
LGSCA, *n* (%)	–	–	8 (23.5)	
HGSCA, *w* (%)	–	–	26 (76.5)	

CA125 – cancer antigen 125, FIGO – International Federation of Gynecology and Obstetrics, HGSCA – high-grade serous cystadenocarcinoma, LGSCA – low-grade serous cystadenocarcinoma, SCA – serous cystadenocarcinoma

** One-way ANOVA test was used to calculate the p-value.*

Demographic data of study participants together with biochemical measurement and tumor characteristics. Data are represented as mean ± SD. CA125 values were only available as descriptive variables: normal (–), moderately (+), and highly (≥ + +) elevated.

Potential biomarker candidates in serous cystadenocarcinoma disease progression

To assess the diagnostic potential of the significant proteins, the expression of each protein across the three groups was represented using a box plot, followed by ROC analysis. When comparing differentially expressed proteins from benign to borderline to SCA tumors, we identified five upregulated proteins (ASS1, CAPS, PPA1, BCAT1, MCM4) and downregulated proteins (MUC5B, SLC4A1, tenascin-XB – TNXB, carbonic anhydrase 1 – CA1, hemoglobin β – HBB), all of which exhibited AUCs ≥ 0.84 (Fig. 2). In addition, nine proteins previously linked to cancer show acceptable sensitivity and specificity in this study (Suppl. File 2, Table S1). To investigate possible proteins that distinguish borderline from LGSCA and LGSCA from HGSCA, a biomarker panel method was used. Each group of proteins had its own combined ROC curve. The upregulation of LGSCA proteins resulted in a combined ROC AUC value of 0.942, 95% CI: 0.774–1, while the AUC value for LGSCA vs. HGSCA was 0.942, CI: 0.774–1.

Protein markers differentiating borderline from low-grade serous cystadenocarcinoma and low-grade serous cystadenocarcinoma from high-grade serous cystadenocarcinoma

To identify protein markers that effectively distinguished between borderline vs. LGSCA and LGSCA vs. HGSCA, we implemented box plots and ROC analysis. CRABP2, MZB1, and BCAM showed significantly higher expression in LGSCA compared to borderline tumors, with AUC values of 0.97, 0.80, and 0.79, respectively (Figs. 3 A, 3 A–II, Suppl. File 2, Table S1). Pyridoxal dependent decarboxylase domain containing 1, GFPT1, and HYOU1 exhibited higher levels in HGSCA compared to LGSCA, with AUC values in the range 0.83–0.98 (Figs. 3 B, 3 B–III, Suppl. File 2, Table S1). Tenascin-XB showed a progressive decrease in expression from benign tumors to HGSCA, with significant differences observed between benign and HGSCA, as well as borderline and HGSCA (Fig. 3 C, Table S1). Conversely, ASS1 displayed a consistent increase in expression from benign tumors through borderline, LGSCA, and HGSCA, marking it as a potential indicator of disease progression.

Ingenuity pathway analysis revealing altered protein expression pathways in serous cystadenocarcinoma progression

In a pairwise comparison of SCA, borderline, and benign tumors, the IPA analysis identified numerous perturbed "canonical pathways" and "diseases and functions" (Suppl. File 3). Functionally, SCA and borderline tumors are biologically related and distinct from benign tumors. Several diseases and functions associated with cell proliferation and viability were more prevalent in SCA and borderline tumors than in benign tumors. Among disease or function annotations containing "apoptosis" and "cell death," we discovered eleven decreases in SCA and three decreases in borderline tumors compared to benign tumors. When compared to benign tumors, seven annotations containing the word "proliferation" were upregulated in SCA and six in borderline. None of these were significantly different between SCA and borderline tumors, implying that SCA and borderline tumors are more similar in terms of these functions. When SCA was compared to borderline tumors, the biological differences were much less pronounced; for example, the "diseases and functions" analysis revealed increased nucleotide metabolism in SCA as well as changes in proteins involved in certain types of cancers. From the perturbed "canonical pathways" we discovered that SCA and borderline tumors had significantly higher levels of RNA synthesis and processing than benign tumors. For example, "RNA polymerase II transcription," "processing of capped intron-containing pre-mRNA" and "processing of capped intronless pre-mRNA" were higher in SCA and borderline tumors compared to benign tumors. Mitochondrial metabolic functions, such as "oxidative phosphorylation"

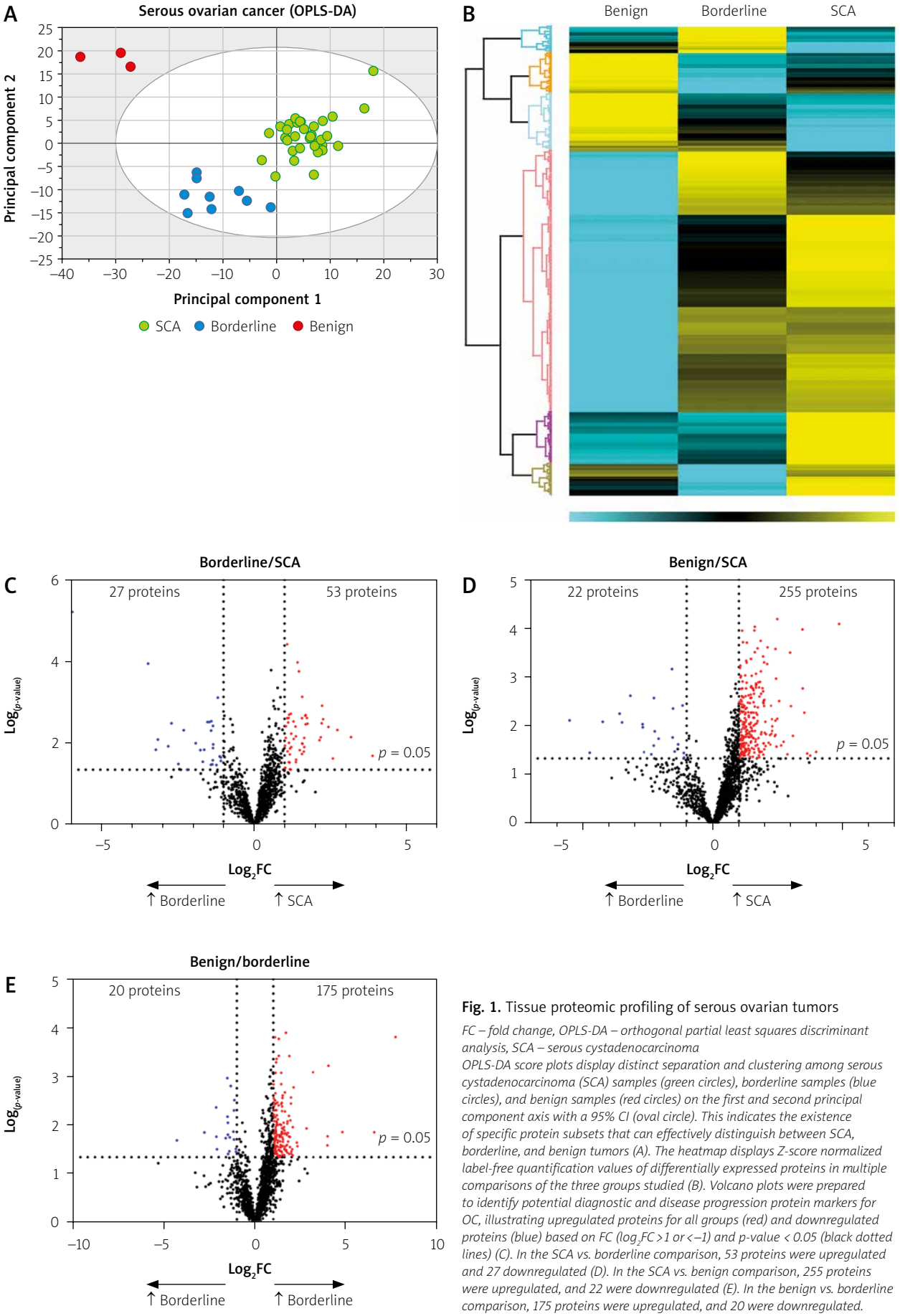

Fig. 1. Tissue proteomic profiling of serous ovarian tumors

FC – fold change, OPLS-DA – orthogonal partial least squares discriminant analysis, SCA – serous cystadenocarcinoma
OPLS-DA score plots display distinct separation and clustering among serous cystadenocarcinoma (SCA) samples (green circles), borderline samples (blue circles), and benign samples (red circles) on the first and second principal component axis with a 95% CI (oval circle). This indicates the existence of specific protein subsets that can effectively distinguish between SCA, borderline, and benign tumors (A). The heatmap displays Z-score normalized label-free quantification values of differentially expressed proteins in multiple comparisons of the three groups studied (B). Volcano plots were prepared to identify potential diagnostic and disease progression protein markers for OC, illustrating upregulated proteins for all groups (red) and downregulated proteins (blue) based on FC ($log_2FC > 1$ or < -1) and p-value < 0.05 (black dotted lines) (C). In the SCA vs. borderline comparison, 53 proteins were upregulated and 27 downregulated (D). In the SCA vs. benign comparison, 255 proteins were upregulated, and 22 were downregulated (E). In the benign vs. borderline comparison, 175 proteins were upregulated, and 20 were downregulated.

Table 2. Top 10 differentially expressed proteins for cystadenocarcinoma/borderline, serous cystadenocarcinoma/benign, and borderline/benign

UniProt ID	Gene name	Protein name	Log_2FC	*p*-value
P20591	*MX1*	SCA/borderline Interferon-induced GTP-binding protein Mx1	3.89	0.021
P54687-4	*BCAT1*	Branched-chain-amino-acid aminotransferase, cytosolic	3.18	0.007
P49736	*MCM2*	DNA replication licensing factor MCM2	2.74	0.005
Q8WU39	*MZB1*	Marginal zone B- and B1-cell-specific protein	2.59	0.025
Q14566	*MCM6*	DNA replication licensing factor MCM6	2.45	0.004
Q03518	*TAP1*	Antigen peptide transporter 1	2.27	0.003
P42224	*STAT1*	Signal transducer and activator of transcription 1-α/β	2.24	0.001
P33991	*MCM4*	DNA replication licensing factor MCM4	2.23	0.003
P33992	*MCM5*	DNA replication licensing factor MCM5	2.19	0.007
P29373	*CRABP2*	Cellular retinoic acid-binding protein 2	2.15	0.009
Q9HC84	*MUC5B*	Mucin-5B	–5.96	0.000
Q9BW30	*TPPP3*	Tubulin polymerization-promoting protein family member 3	–3.47	0.000
P22105-1	*TNXB*	Tenascin-X	–3.21	0.015
P48594	*SERPINB4*	Serpin B4	–3.15	0.008
Q13938-4	*CAPS*	Calcyphosin	–2.81	0.012
O60437	*PPL*	Periplakin	–2.70	0.003
P20774	*OGN*	Mimecan	–2.48	0.034
P58107	*EPPK1*	Epiplakin	–2.44	0.046
Q7L266	*ASRGL1*	Isoaspartyl peptidase	–2.30	0.005
SCA/benign				
P00966	*ASS1*	Argininosuccinate synthase	4.85	0.000
P54687-4	*BCAT1*	Branched-chain-amino-acid aminotransferase, cytosolic	3.97	0.034
Q13938-4	*CAPS*	Calcyphosin	3.75	0.041
Q96RQ9	*IL4I1*	L-amino-acid oxidase	3.63	0.037
P42704	*LRPPRC*	Leucine-rich PPR motif-containing protein, mitochondrial	3.52	0.005
P50895	*BCAM*	Basal cell adhesion molecule	3.46	0.002
Q15181	*PPA1*	Inorganic pyrophosphatase	3.45	0.000
P33991	*MCM4*	DNA replication licensing factor MCM4	3.08	0.016
P43304-2	*GPD2*	Glycerol-3-phosphate dehydrogenase, mitochondrial	3.01	0.004
P55327-2	*TPD52*	Tumor protein D52	2.97	0.000
P02730	*SLC4A1*	Band 3 anion transport protein	–5.50	0.008
P22105-1	*TNXB*	Tenascin-X	–4.73	0.036
P01266	*TG*	Thyroglobulin	–4.23	0.008
P02042	*HBD*	Hemoglobin subunit delta	–3.58	0.006
P00915	*CA1*	Carbonic anhydrase 1	–3.49	0.009
P68871	*HBB*	Hemoglobin subunit β	–3.17	0.002
P69905	*HBA1*	Hemoglobin subunit α	–2.70	0.009
Q16647	*PTGIS*	Prostacyclin synthase	–2.69	0.011
P04275	*VWF*	von Willebrand factor	–2.64	0.035
Borderline/benign				
Q9HC84	*MUC5B*	Mucin-5B	7.73	0.000
Q13938-4	*CAPS*	Calcyphosin	6.56	0.014
P58107	*EPPK1*	Epiplakin	4.82	0.014
Q7L266	*ASRGL1*	Isoaspartyl peptidase	4.05	0.001
Q9BW30	*TPPP3*	Tubulin polymerization-promoting protein family member 3	4.01	0.017
O60437	*PPL*	Periplakin	3.99	0.027

Table 2. Cont.

UniProt ID	Gene name	Protein name	Log_2FC	*p*-value
P00966	*ASS1*	Argininosuccinate synthase	3.20	0.001
Q15181	*PPA1*	Inorganic pyrophosphatase	2.82	0.012
Q6P2Q9	*PRPF8*	Pre-mRNA-processing-splicing factor 8	2.33	0.028
P15941-7	*MUC1*	Mucin-1	2.29	0.023
P24821	*TNC*	Tenascin	–4.31	0.021
Q16647	*PTGIS*	Prostacyclin synthase	–2.77	0.015
P02751-3	*FN1*	Fibronectin	–2.13	0.004
Q53GG5-2	*PDLIM3*	PDZ and LIM domain protein 3	–2.11	0.018
P07942	*LAMB1*	Laminin subunit β -1	–2.08	0.032
Q99715	*COL12A1*	Collagen α-1(XII) chain	–1.61	0.019
P11215	*ITGAM*	Integrin α-M	–1.52	0.001
Q02809	*PLOD1*	Procollagen-lysine,2-oxoglutarate 5-dioxygenase 1	–1.50	0.007
Q8IUX7	*AEBP1*	Adipocyte enhancer-binding protein 1	–1.48	0.016
P05997	*COL5A2*	Collagen α-2(V) chain	–1.48	0.009

ASS1 – argininosuccinate synthase 1, FC – fold change, HBB – hemoglobin β, SCA – serous cystadenocarcinoma, TNX – tenascin-X
A log_2FC ±1 indicates a two-fold increase (+) or decrease (–) in serous cystadenocarcinoma/borderline, serous cystadenocarcinoma/benign and borderline/benign.

were higher in SCA compared to borderline tumors. Serous cystadenocarcinoma and borderline tumors were distinct, despite being biologically closely related, with some differences in nucleotide and mitochondrial metabolic processes. Both tumors exhibit high proliferation, distinguishing them from benign tumors.

Discussion

Serous ovarian tumors are complex and heterogeneous groups of neoplasms, encompassing various entities from benign *via* borderline and LGSCA to high-grade neoplasms, such as HGSCA. The most common, HGSCA, is also the deadliest gynecological cancer, and early detection is vital for enhanced patient outcomes. Therefore, identifying new biomarkers that can enhance diagnostic capabilities independently or in combination with existing tumor markers is essential. This study presents an extensive proteomic analysis of FFPE tissue samples obtained at the time of diagnosis from benign tumors, borderline tumors, and SCA. Our study aimed to identify tissue-based markers associated with disease development and progression to provide potential targets for future research and therapeutic interventions.

We conducted a detailed comparison of protein profiles across three ovarian tumor conditions: SCA vs. borderline (n = 80), SCA vs. benign (n = 277), and borderline vs. benign (n = 195), as depicted in Figs. 1 C–E and detailed in Supplementary File 1. This analysis also highlighted significant differences, including the upregulation and downregulation of the top ten proteins between SCA vs. benign, SCA vs. benign, and borderline vs. benign (Table 2). Our comparative analysis of protein expression across benign, borderline, and SCA tumors indicated that five proteins (ASS1, CAPS, PPA1, BCAT1, MCM4) were significantly upregulated, while five proteins (MUC5B, SLC4A1, TNXB, CA1, HBB) were downregulated. All of these proteins exhibited AUCs ≥ 0.84. PPA1 overexpression, linked to poor survival and chemoresistance, impacts key oncogenic pathways such as p53, β-catenin, and PI3K/AKT/GSK3 [51, 52]. Argininosuccinate synthase 1, pivotal in arginine metabolism, is overexpressed in HGSCA facilitating tumor growth and metastasis, possibly modulated *via* the IL-17/CXCL8 pathway [53]. Moreover, CAPS, BCAT1, and MCM4 distinctly differentiate between SCA and benign tumors, suggesting their potential utility in diagnostics. Further insights include BCAT1 in promoting proliferation and invasion in epithelial ovarian cancer, correlating with poor outcomes [54, 55]. The expression of MCM4 is closely tied to the cancer stage and presents high predictive value in ovarian cancer diagnostics [56]. Conversely, CAPS, though prevalent in lung and colorectal cancers, has an uncertain role in ovarian cancer pathology [57]. Significant downregulations noted in our study, such as MUC5B, a glycoprotein with varied expression in gastric and breast cancers, show reduced levels in higher-grade ovarian tumors, aligning with our findings of lower MUC5B in SCA than borderline tumors [57]. These molecular distinctions offer a deeper understanding of ovarian cancer pathology and could guide future therapeutic strategies [58].

Carbonic anhydrases control respiration, pH, and ion transport [59, 60]. Carbonic anhydrases influence the pH levels of cancer cells and their surrounding microenvironment. These pH changes influence the ability of tumors to evade the immune system, proliferate, and invade nearby tissues. Carbonic anhydrase 1 level changes have been linked to several cancers, including colorectal cancer, myeloid leukemia, and renal carcinoma, and they have been proposed as a biomarker for non-small lung cancer [59, 60]. Hemoglobin β transports oxygen within erythrocytes, facilitating cellular respiration and maintaining metabolic balance. Recent cancer research has revealed aberrant expression in a variety of malignancies. For example, HBB has been identified as a lung-derived antimetastatic factor that inhibits neuroblastoma growth and metastasis, and anoth-

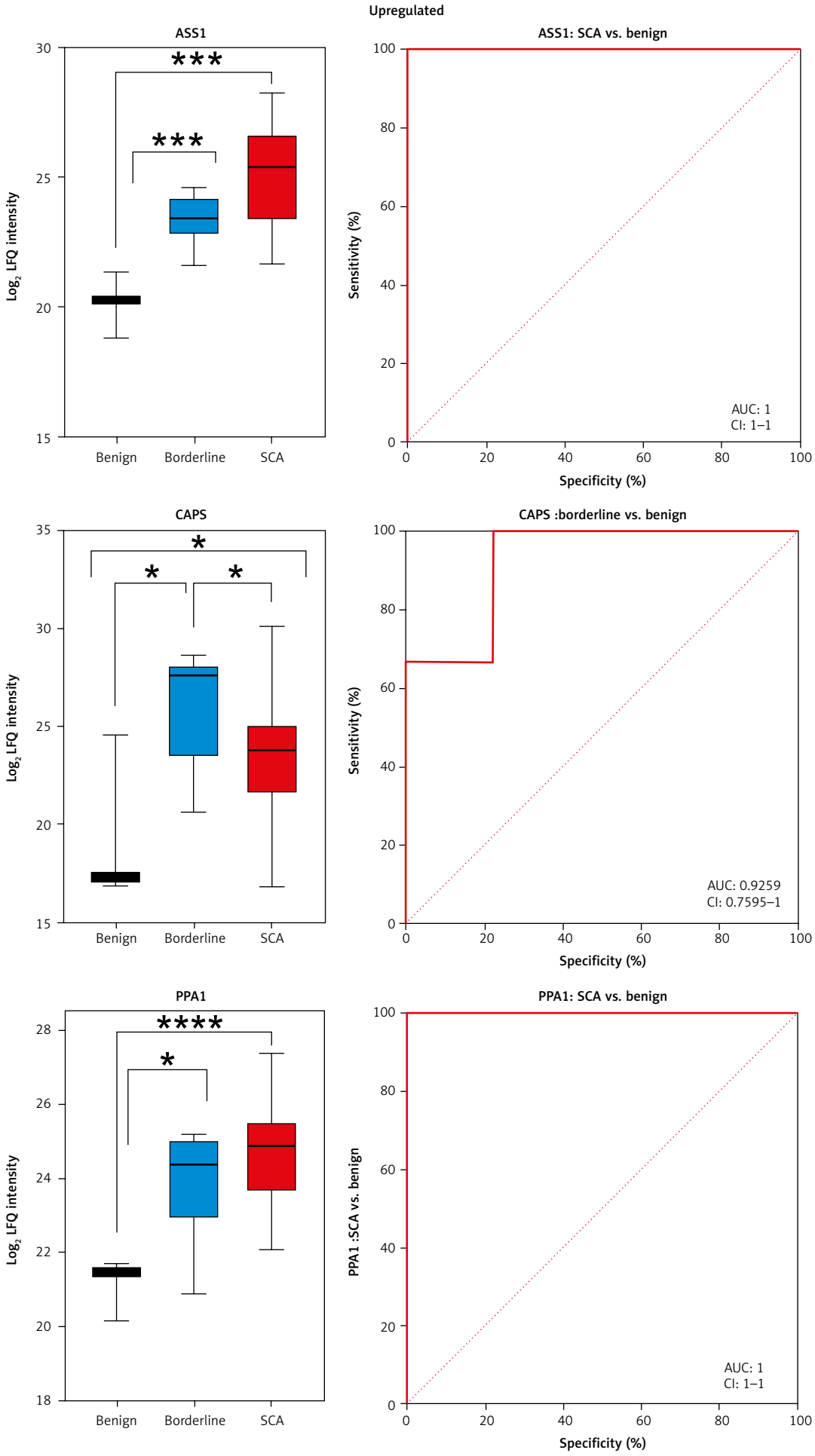

Fig. 2. Identification of disease progression biomarkers in serous ovarian cancer

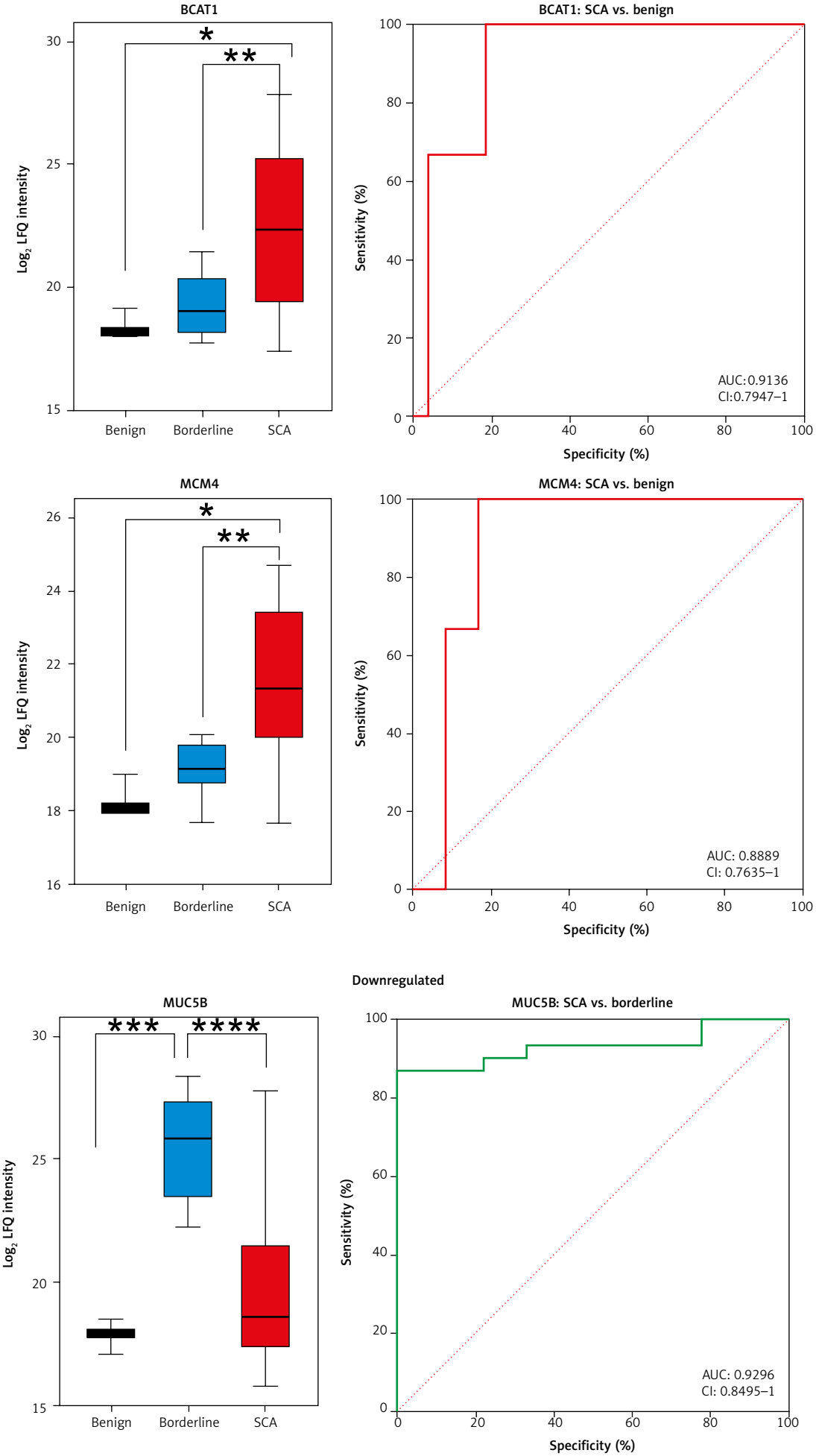
BCAT1
Log2 LFQ intensity
Benign
Borderline
SCA
BCAT1: SCA vs. benign
Sensitivity (%)
Specificity (%)
AUC: 0.9136
CI: 0.7947–1
MCM4
MCM4: SCA vs. benign
AUC: 0.8889
CI: 0.7635–1
Downregulated
MUC5B
MUC5B: SCA vs. borderline
AUC: 0.9296
CI: 0.8495–1

Fig. 2. Cont.

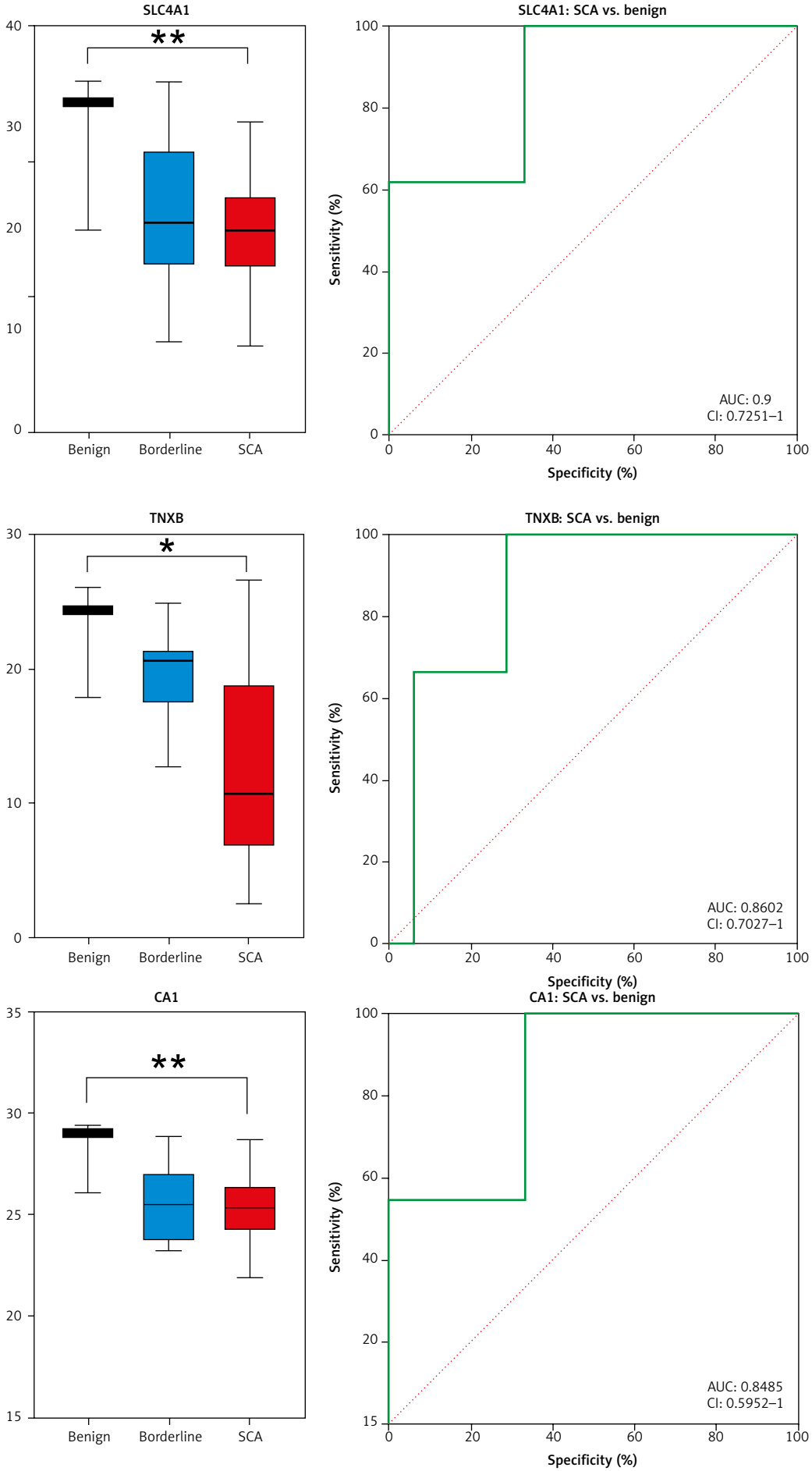
SLC4A1
**
Benign
Borderline
SCA
SLC4A1: SCA vs. benign
Sensitivity (%)
Specificity (%)
AUC: 0.9
CI: 0.7251–1
TNXB
*
TNXB: SCA vs. benign
AUC: 0.8602
CI: 0.7027–1
CA1
**
CA1: SCA vs. benign
AUC: 0.8485
CI: 0.5952–1

Fig. 2. Cont.

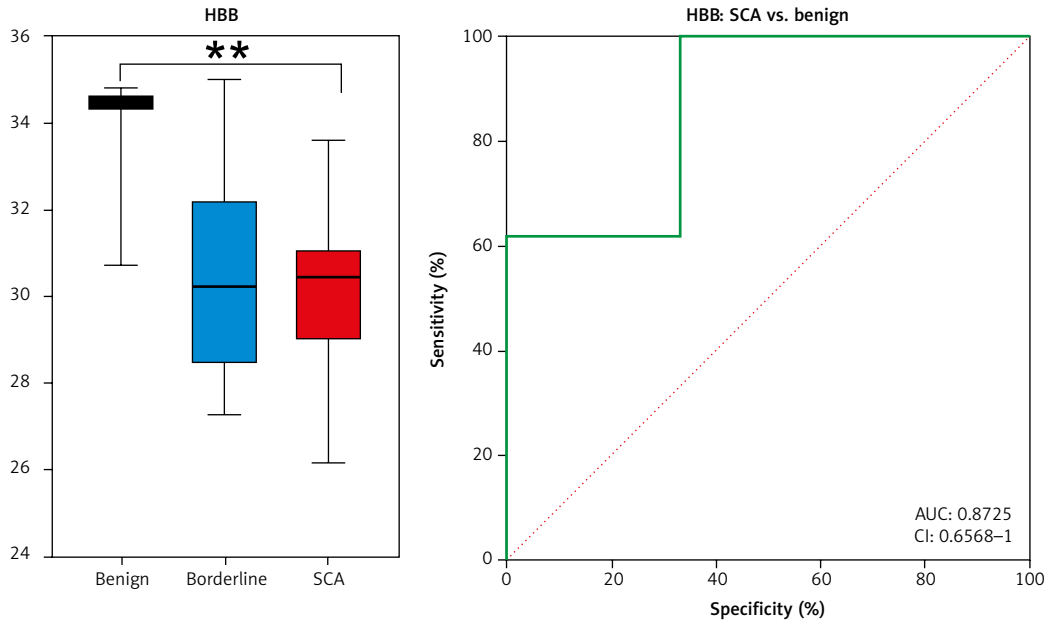

Fig. 2. Cont.

AUC – area under the curve, ASS1 – argininosuccinate synthetase 1, BCAT1 – branched chain amino acid transaminase, CA1 – carbonic anhydrase 1, CAPS – calcyphosin, CI – confidence interval, HBB – hemoglobin β, LFQ – label-free quantification, MCM4 – minichromosome maintenance complex component 4, while proteins exhibiting reduced expression were MUC5B – mucin-5B, PPA1 – inorganic pyrophosphatase 1, SCA – serous cystadenocarcinoma, SLC4A1 – solute carrier family 4 member 1, TNXB – tenascin-XB

Receiver operating characteristic curves and box plots of protein candidates. Proteins exhibiting increased expression in the serous cystadenocarcinoma, which hold diagnostic potential. Box plots display logarithmic label-free quantification intensities excluding NaN (missing values).

**** p < 0.001*

***** p < 0.0001*

er study highlighted its potential as a serum biomarker for ovarian cancer due to elevated levels in patient sera [61–63]. In contrast, our findings show significant down-regulation of HBB expression between benign tumors and SCA, indicating that HBB plays a different role that may be specific to the tumor type or stage. While the exact role of SCL4A1 in ovarian cancer is unknown, high SLC4A1 expression has been associated with poor progression-free survival [64].

Our study accentuates the diagnostic potential of specific protein markers in distinguishing between SCA, borderline, and benign tumors. Moreover, our identification of upregulated and downregulated proteins provides insights into ovarian cancer progression and highlights potential avenues for further research and therapeutic intervention. Moreover, we further explored the role of ASS1 and TNXB as disease progression markers in SCA. The progressive increase in ASS1 expression from benign to borderline to malignant tumors suggests a potential role in ovarian cancer progression. Argininosuccinate synthase 1 is involved in the urea cycle and arginine biosynthesis, and its upregulation may support the increased metabolic demands of rapidly proliferating cancer cells [65]. There is strong crosstalk between constituents of the urea cycle and other metabolic pathways which have been shown to promote tumorigenesis in various cell types [66]. Recent studies have linked ASS1 to the IL-17/CXCL8 signaling pathway in ovarian cancer, potentially contributing to tumor growth and metastasis [66] For other types of cancer, ASS1 has been shown to have decreased expression, and this decrease has been associated with increased cancer cell survival, migration, and invasion [67]. However, in ovarian cancer, it has been documented that increased expression of ASS1 is present. Specifically, increased expression of ASS1 is seen in LGSCA and HGSCA [68]. Interestingly, similarly to other cancers, a decrease of ASS1 expression was found in non-serous ovarian cancer subtypes [66]. Our findings corroborate existing literature by showing a progressive increase in ASS1 expression across our samples. Additionally, we observed a novel trend: ASS1 expression begins to increase from the borderline stage of tumor development in SCA, a pattern not previously reported.

In contrast, TNXB, an extracellular matrix glycoprotein that is predominantly expressed during embryogenesis, showed a progressive decrease from benign to malignant tumors in our study [69, 70]. This is consistent with previous findings in other cancer types, where TNXB loss has been linked to tumor progression [71]. Tenascin-XB may play a role in maintaining tissue integrity, and its loss could facilitate tumor invasion and metastasis [72, 73]. Our observation of decreased TNXB levels in ovarian tumors contrasts with a previous study by Marcišauskas *et al.*, which reported increased TNXB in ovarian cancer cyst fluid [74]. This discrepancy could be due to differences in sample types (tissue vs. cyst fluid), tumor heterogeneity, or variations in protein processing and secretion. Further investigation is needed to reconcile these findings and understand the complex role of TNXB in ovarian cancer biology.

The identification of differentially expressed proteins from tumor tissue presents significant potential for future clinical applications in the early diagnosis and molecular typing of ovarian cancer. Our study highlights several key proteins, such as ASS1 and TNXB, which serve as biomarkers for distinguishing between benign, borderline, and SCA while providing insights into disease progression. The robust

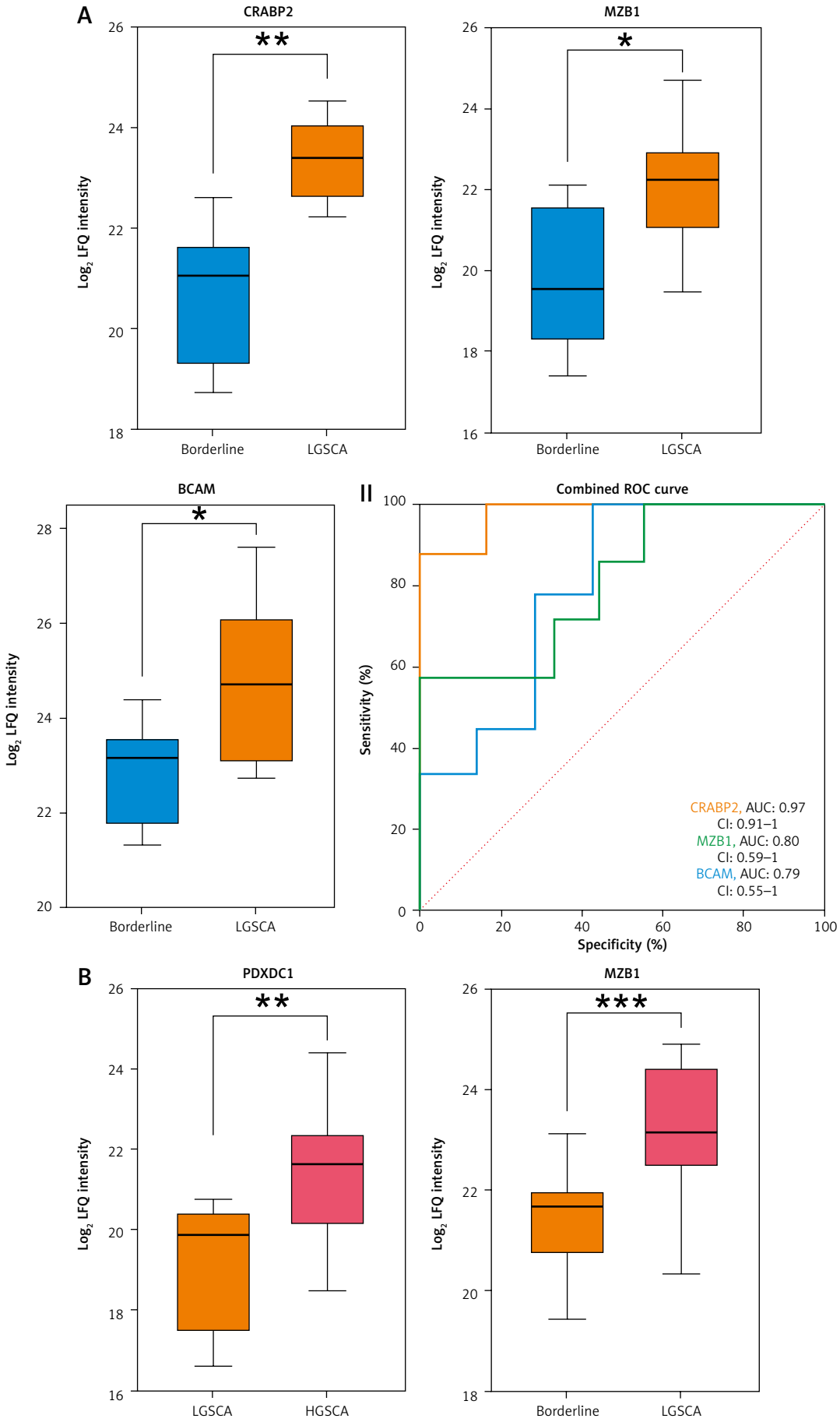

Fig. 3. Highlights the identification of protein markers capable of differentiating borderline from low-grade serous cystadenocarcinoma (LGSCA) and LGSCA from high-grade serous cystadenocarcinoma

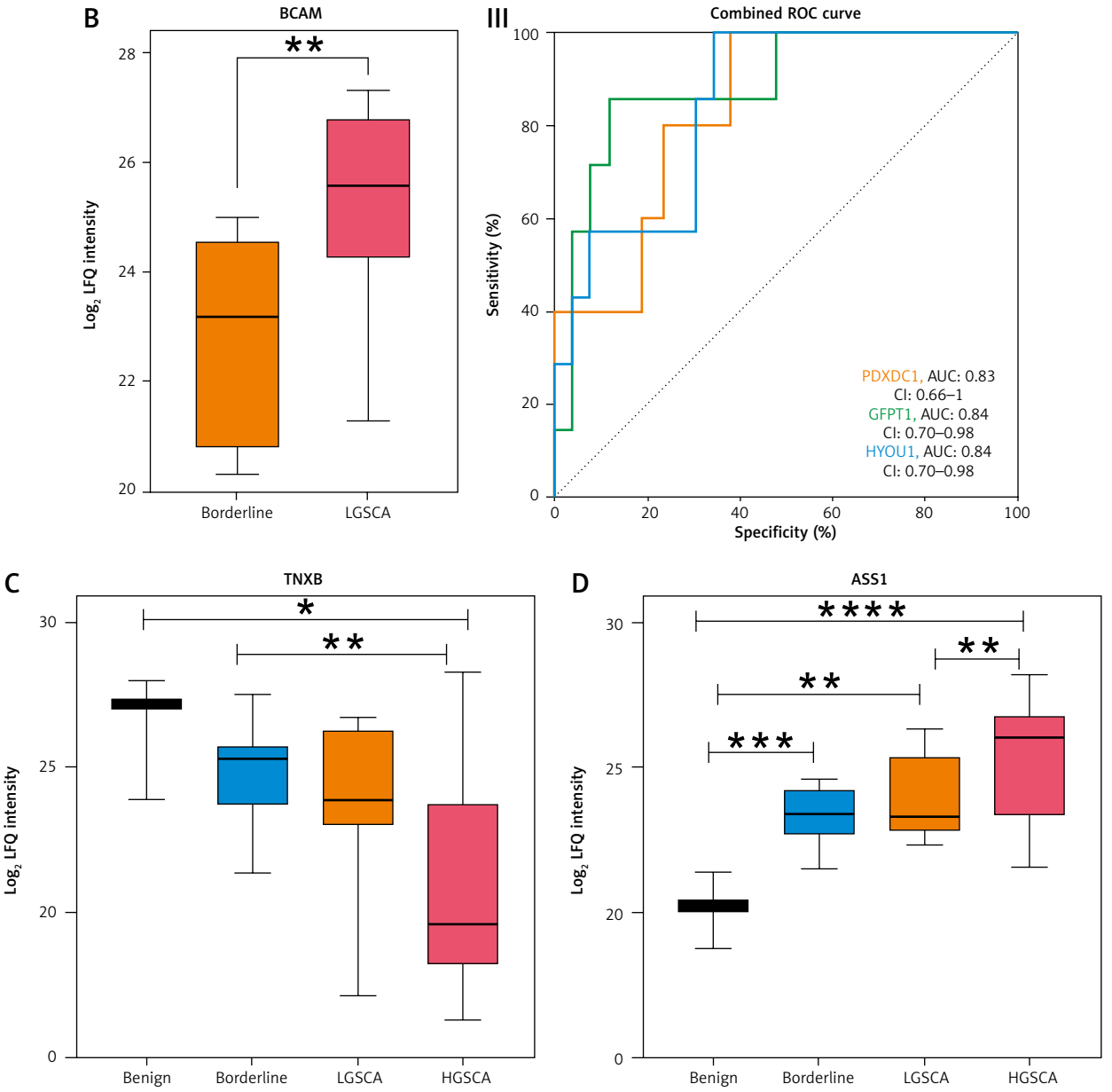

Fig. 3. Cont.

AUC – area under the curve, CI – confidence interval, LGSCA – low-grade serous cystadenocarcinoma, HGSCA – high-grade serous cystadenocarcinoma, LFQ – label-free quantification

*Box plots of three possible protein biomarkers for borderline to LGSCA progression. Comparing borderline tumors to LGSCA reveals a significant increase in levels of CRABP2 – cellular retinoic acid-binding protein 2, MZB1 – marginal zone B and B1 cell specific protein, and BCAM – basal cell adhesion molecule (**A**). Box plots of three potential protein biomarkers for identifying LGSCA and high-grade serous cystadenocarcinoma (HGSCA) (**B**). Levels of PDXDC1 – pyridoxal dependent decarboxylase domain containing 1, GFPT1 – glutamine-fructose-6-phosphate transaminase 1, and HYOU1 – hypoxia up-regulated 1 were significantly increased. ROC curves for distinguishing between borderline and LGSCA proteins, and ROC curves (III) for proteins that distinguish LGSCA from HGSCA (II). Box plots of tenascin-XB (TNXB) and argininosuccinate synthase 1 (ASS1) as potential serous cystadenocarcinoma disease progression markers (**C, D**). For TNXB, there is a progressive decrease from benign to HGSCA, with significant differences between benign and HGSCA, as well as borderline and HGSCA. A significant progressive change can be seen in log_2 label-free quantification intensities of ASS1 from benign to borderline, LGSCA, and HGSCA (Fig. 3 C, Suppl. File 2, Table S1).*

** p < 0.05*

*** p < 0.01*

**** p < 0.001*

***** p < 0.0001*

protein profiles identified through our proteomic analysis present potential to facilitate the development of diagnostic assays aimed at enhancing early detection, which is critical given the often asymptomatic nature of ovarian cancer in its initial stages. Furthermore, classifying tumors based on their molecular characteristics could enable personalized treatment strategies, allowing clinicians to tailor interventions according to individual protein expression profiles. This aligns with the growing trend toward precision medicine in oncology, where understanding the unique biological landscape of a patient's tumor can significantly improve outcomes. By integrating these biomarkers into clinical practice, we could enhance diagnostic accuracy and improve monitoring of disease progression, ultimately contributing

to better patient management and survival rates in ovarian cancer. The identified biomarkers, such as ASS1 and TNXB, should also be further validated using some of the ancillary diagnostic techniques, including immunohistochemistry.

While our study provides valuable insights into potential biomarkers for ovarian cancer progression, several limitations must be considered. The small sample size, particularly for benign (n = 3) and borderline (n = 9) tumors, substantially limits the statistical power and generalizability of our findings. Additionally, the lack of an independent validation cohort means that our results should be considered preliminary and require further confirmation. Additionally, there is a lack of quantitative CA125 data available for correlation, which limits our ability to explore potential relationships. Moreover, the number of patients with advanced stage cancer is limited, with only three patients included, further constraining the analysis. Regarding the methodology employed, the MS datasets contain numerous instances of missing data, potentially resulting in the loss of important comparisons. Missing values may be due to protein levels below the detection limit or technical limitations. Due to limited sample availability, we opted for the well-established data-dependent acquisition technique, which yields similar peptide and protein quantification [75, 76]. To address missing values, we employed the "match between runs" option in MaxQuant analysis, as recommended by Yu *et al*. [77]. Determining data filtration stringency is subjective; overly strict methods risk overlooking important markers, while no filtration may introduce contaminants and biased results.

MS

Conclusions

Our preliminary study provides an understanding of protein expression patterns in ovarian tumors and their relevance for diagnostics and treatment. Through our MS-based tissue proteomics analysis, we have identified promising protein pathways and biomarkers associated with SCA. The expression of these biomarkers shows correlations with tumor progression, from benign and borderline tumors to LGSCA and HGSCA. These findings shed light on the mechanisms underlying ovarian carcinogenesis, emphasizing the need for further investigation and validation of these biomarkers with clinical markers such as CA125 and HE4 to determine whether they offer complementary or superior diagnostic value. Further diagnostic and clinical studies should be performed to confirm the validity and clinical utility of the identified biomarkers.

Disclosures

1. This paper will be supported by Qatar University, College of Medicine, QU Health Cluster.

All samples were collected in the private pathology laboratory in Aleppo, Syria. In line with the local ethical standards of Syrian pathologists, practicing physicians orally informed cancer patients about the potential utilization of their samples in research. Hence, written informed consent and approval were not required. All samples were de-identified and anonymized for study purposes. All data generated or analyzed during this study are included in this published article (and its supplementary information files).

2. The authors of this study express their gratitude to Dr. Ishita Gupta and Mona Britt Hansen for their invaluable assistance in preparing the tissue samples for analysis. BH is grateful to A. P. Møller and Hustru Chastine Mc-Kinney Møllers Fond til almene Fomaal for funding the Orbitrap Fusion Tribrid mass spectrometer.

3. Financial support and sponsorship: None.

4. Conflicts of interest: None.

References

1. Yahata T, Banzai C, Tanaka K. Histology-specific long-term trends in the incidence of ovarian cancer and borderline tumor in Japanese females: a population-based study from 1983 to 2007 in Niigata. J Obstet Gynaecol Res 2012; 38: 645-650.
2. Reid BM, Permuth JB, Sellers TA. Epidemiology of ovarian cancer: a review. Cancer Biol Med 2017; 14: 9-32.
3. Huang J, Chan WC, Ngai CH, et al. Worldwide burden, risk factors, and temporal trends of ovarian cancer: a global study. Cancers (Basel) 2022; 14: 2230.
4. Siegel R, Naishadham D, Jemal A. Cancer statistics, 2012. CA Cancer J Clin 2012; 62: 10-29.
5. Jelovac D, Armstrong DK. Recent progress in the diagnosis and treatment of ovarian cancer. CA Cancer Clin 2011; 61: 183-203.
6. Köbel M, Kalloger SE, Boyd N, et al. Ovarian carcinoma subtypes are different diseases: implications for biomarker studies. PLoS Med 2008; 5: e232-e.
7. Lheureux S, Braunstein M, Oza AM. Epithelial ovarian cancer: evolution of management in the era of precision medicine. CA Cancer J Clin 2019; 69: 280-304.
8. Hayashi T, Konishi I. Molecular histopathology for establishing diagnostic method and clinical therapy for ovarian carcinoma. J Clin Med Res 2023; 15: 68-75.
9. Kurman RJ, Shih IM. The origin and pathogenesis of epithelial ovarian cancer: a proposed unifying theory. Am J Surg Pathol 2010; 34: 433-443.
10. Kurman RJ, Shih IM. Molecular pathogenesis and extraovarian origin of epithelial ovarian cancer – shifting the paradigm. Hum Pathol 2011; 42: 918-931.
11. Tsuboyama T, Sato K, Ota T, et al. MRI of borderline epithelial ovarian tumors: pathologic correlation and diagnostic challenges. RadioGraphics 2022; 42: 2095-2111.
12. Malpica A, Deavers MT, Lu K, et al. Grading ovarian serous carcinoma using a two-tier system. Am J Surg Pathol 2004; 28: 496-504.
13. Seidman JD, Savage J, Krishnan J, Vang R, Kurman RJ. Intratumoral heterogeneity accounts for apparent progression of noninvasive serous tumors to invasive low-grade serous carcinoma: a study of 30 low-grade serous tumors of the ovary in 18 patients with peritoneal carcinomatosis. Int J Gynecol Pathol 2020; 39: 43-54.
14. Geomini P, Bremer G, Kruitwagen R, Mol BWJ. Diagnostic accuracy of frozen section diagnosis of the adnexal mass: a metaanalysis. Gynecol Oncol 2005; 96: 1-9.
15. Jagelkova M, Zelinova K, Laucekova Z, et al. Comparison of somatic mutation profiles between formalin-fixed paraffin embedded tissues and plasma cell-free dna from ovarian cancer patients before and after surgery. Biores Open Access 2020; 9: 73-79.
16. Gee ME, Faraahi Z, McCormick A, Edmondson RJ. DNA damage repair in ovarian cancer: unlocking the heterogeneity. J Ovarian Res 2018; 11: 50.
17. Rebbeck TR, Mitra N, Wan F, et al. Association of type and location of BRCA1 and BRCA2 mutations with risk of breast and ovarian cancer. JAMA 2015; 313: 1347-1361.
18. Kurman RJ, Shih IM. The dualistic model of ovarian carcinogenesis: revisited, revised, and expanded. Am J Patho. 2016; 186: 733-747.
19. Landen CN, Birrer MJ, Sood AK. Early events in the pathogenesis of epithelial ovarian cancer. J Clin Oncol 2008; 26: 995-1005.

20. Seidman JD, Horkayne-Szakaly I, Haiba M, Boice CR, Kurman RJ, Ronnett BM. The histologic type and stage distribution of ovarian carcinomas of surface epithelial origin. Int J Gynecol Pathol 2004; 23: 41-44.
21. Sandri MT, Bottari F, Franchi D, et al. Comparison of HE4, CA125 and ROMA algorithm in women with a pelvic mass: Correlation with pathological outcome. Gynecol Oncol 2013; 128: 233-238.
22. Granato T, Porpora MG, Longo F, Angeloni A, Manganaro L, Anastasi E. HE4 in the differential diagnosis of ovarian masses. Clin Chim Acta 2015; 446: 147-155.
23. Prueksaritanond N, Angsathapon S, Insin P. The utility of preoperative serum CA125 combined with HE4 to predict lymph node metastasis in endometrial cancer. Gynecol Obstet Invest 2023; 88: 53-60.
24. Kotowicz BU, Fuksiewicz M, Bidzinski M, Berezowska A, Sobiczewski P, Kowalska MM. Measurement of HE4 six months after first-line treatment as optimal time in identifying patients at high risk of progression advanced ovarian cancer. Ginekol Pol 2022; 93: 910-915.
25. Zhang R, Siu MKY, Ngan HYS, Chan KKL. Molecular Biomarkers for the early detection of ovarian cancer. Int J Mol Sci 2022; 23: 12041.
26. Sugiyama T, Nishida T, Komai K, Nishimura H, Yakushiji M, Nishimura H. Comparison of CA 125 assays with abdominopelvic computed tomography and transvaginal ultrasound in monitoring of ovarian cancer. Int J Gynecol Obstet 1996; 54: 251-256.
27. Kumari S. Serum biomarker based algorithms in diagnosis of ovarian cancer: a review. Indian J Clin Biochem 2018; 33: 382-386.
28. Fritsche HA, Bullock RG. A reflex testing protocol using two multivariate index assays improves the risk assessment for ovarian cancer in patients with an adnexal mass. Int J Gynecol Obstet 2023; 162: 485-492.
29. Yang S, Tang J, Rong Y, et al. Performance of the IOTA ADNEX model combined with HE4 for identifying early-stage ovarian cancer. Front Oncol 2022; 12: 949766.
30. Karlsen MA, Sandhu N, Høgdall C, et al. Evaluation of HE4, CA125, risk of ovarian malignancy algorithm (ROMA) and risk of malignancy index (RMI) as diagnostic tools of epithelial ovarian cancer in patients with a pelvic mass. Gynecol Oncol 2012; 127: 379-383.
31. Romagnolo C, Leon AE, Fabricio ASC, et al. HE4, CA125 and risk of ovarian malignancy algorithm (ROMA) as diagnostic tools for ovarian cancer in patients with a pelvic mass: An Italian multicenter study. Gynecol Oncol 2016; 141: 303-311.
32. Davenport C, Rai N, Sharma P, et al. Menopausal status, ultrasound and biomarker tests in combination for the diagnosis of ovarian cancer in symptomatic women. Cochrane Database Syst Rev 2022; 7: CD011964-CD.
33. Ueland FR. A perspective on ovarian cancer biomarkers: past, present and yet-to-come. Diagnostics (Basel) 2017; 7: 14.
34. Swiatly A, Horala A, Hajduk J, Matysiak J, Nowak-Markwitz E, Kokot ZJ. MALDI-TOF-MS analysis in discovery and identification of serum proteomic patterns of ovarian cancer. BMC Cancer 2017; 17: 472.
35. Sobsey CA, Ibrahim S, Richard VR, et al. Targeted and untargeted proteomics approaches in biomarker development. PROTEOMICS. 2020; 20: e1900029.
36. Noreen S, Gardner QA, Fatima I, Sadaf S, Akhtar MW. Upregulated expression of calcium-dependent annexin a6: a potential biomarker of ovarian carcinoma. PROTEOMICS Clin Appl 2020; 14: e1900078.
37. Huang D, Gaul DA, Nan H, Kim J, Fernández FM. Deep metabolomics of a high-grade serous ovarian cancer triple-knockout mouse model. J Proteome Res 2019; 18: 3184-3194.
38. Bockorny B, Muthuswamy L, Huang L, et al. A Large-scale proteomics resource of circulating extracellular vesicles for biomarker discovery in pancreatic cancer. eLife Sciences Publications, Ltd, Cambridge 2023.
39. Kim D, Gupta B, Wong GYM. Prognostic circulating proteomic biomarkers in colorectal liver metastases. Comput Struct Biotechnol J 2023; 21: 2129-2136.
40. Pedersen S, Jensen KP, Honoré B, et al. Circulating microvesicles and exosomes in small cell lung cancer by quantitative proteomics. Clin Proteomics 2022; 19: 2.
41. Islam Khan MZ, Tam SY, Law HKW. Advances in high throughput proteomics profiling in establishing potential biomarkers for gastrointestinal cancer. Cells 2022; 11: 973.
42. Delcourt V, Franck J, Leblanc E, et al. Combined mass spectrometry imaging and top-down microproteomics reveals evidence of a hidden proteome in ovarian cancer. EBioMedicine 2017; 21: 55-64.
43. Penick ER, Bateman NW, Rojas C, et al. Proteomic alterations associated with residual disease in neoadjuvant chemotherapy treated ovarian cancer tissues. Clin Proteomics 2022; 19: 35.
44. Shrestha R, Llaurado Fernandez M, Dawson A, et al. Multiomics characterization of low-grade serous ovarian carcinoma identifies potential biomarkers of MEK inhibitor sensitivity and therapeutic vulnerability. Cancer Res 2021; 81: 1681-1694.
45. Honoré B. Proteomic protocols for differential protein expression analyses. Xenotransplantation: Springer US 2020, 47-58.
46. Cehofski LJ, Kojima K, Terao N, et al. Aqueous fibronectin correlates with severity of macular edema and visual acuity in patients with branch retinal vein occlusion: a proteome study. Invest Ophthalmol Vis Sci 2020; 61: 6.
47. Tyanova S, Temu T, Cox J. The MaxQuant computational platform for mass spectrometry – based shotgun proteomics. Nature Protocols 2016; 11: 2301-2319.
48. Christakopoulos C, Cehofski LJ, Christensen SR, Vorum H, Honoré B. Proteomics reveals a set of highly enriched proteins in epiretinal membrane compared with inner limiting membrane. Exp Eye Res 2019; 186: 107722.
49. Cox J, Hein MY, Luber CA, Paron I, Nagaraj N, Mann M. Accurate proteome-wide label-free quantification by delayed normalization and maximal peptide ratio extraction, termed MaxLFQ. Mol Cell Proteomics 2014; 13: 2513-2526.
50. Krämer A, Green J, Pollard J Jr., Tugendreich S. Causal analysis approaches in ingenuity pathway analysis. Bioinformatics 2014; 30: 523-530.
51. Guo C, Li S, Liang A, Cui M, Lou Y, Wang H. PPA1 promotes breast cancer proliferation and metastasis through PI3K/AKT/GSK3βsignaling pathway. Front Cell Dev Biol 2021; 9: 730558.
52. Li H, Xiao N, Li Z, Wang Q. Expression of inorganic pyrophosphatase (PPA1) correlates with poor prognosis of epithelial ovarian cancer. Tohoku J Exp Med 2017; 241: 165-173.
53. Feng X, Ji Z, Yang G. ASS1 regulates immune microenvironment via CXCL8 signaling in ovarian cancer. Biochem Biophys Res Commun 2022; 631: 86-92.
54. Nong X, Zhang C, Wang J, Ding P, Ji G, Wu T. The mechanism of branched-chain amino acid transferases in different diseases: Research progress and future prospects. Front Oncol 2022; 12: 988290.
55. Li GS, Huang HQ, Liang Y, et al. BCAT1: a risk factor in multiple cancers based on a pan-cancer analysis. Cancer Med 2022; 11: 1396-1412.
56. Li Y, Gao W, Yang Z, Hu Z, Li J. Multi-omics pan-cancer analyses identify MCM4 as a promising prognostic and diagnostic biomarker. Sci Rep 2024; 14: 6517.
57. Shao W, Wang Q, Wang F, Jiang Y, Xu M, Xu J. Abnormal expression of calcyphosine is associated with poor prognosis and cell biology function in colorectal cancer. Onco Targets Ther 2016; 9: 477-487.
58. Partheen K, Levan K, Osterberg L, Horvath G. Expression analysis of stage III serous ovarian adenocarcinoma distinguishes a sub-group of survivors. Eur J Cancer 2006; 42: 2846-2854.
59. Wang DB, Lu XK, Zhang X, Li ZG, Li CX. Carbonic anhydrase 1 is a promising biomarker for early detection of non-small cell lung cancer. Tumour Biol 2016; 37: 553-559.
60. Becker HM. Carbonic anhydrase IX and acid transport in cancer. Br J Cancer 2020; 122: 157-167.
61. Kurota Y, Takeda Y, Ichiyanagi O, et al. Hemoglobin beta expression is associated with poor prognosis in clear cell renal cell carcinoma. Biomedicines 2023; 11: 1330.
62. Maman S, Sagi-Assif O, Yuan W, et al. The beta subunit of hemoglobin (HBB2/HBB) suppresses neuroblastoma growth and metastasis. Cancer Res 2017; 77: 14-26.
63. Woong-Shick A, Sung-Pil P, Su-Mi B, et al. Identification of hemoglobin-alpha and -beta subunits as potential serum biomarkers for the diagnosis and prognosis of ovarian cancer. Cancer Sci 2005; 96: 197-201.
64. Schilling V, Beyerlein P, Chien J. A Bioinformatics analysis of ovarian cancer data using machine learning. Algorithms 2023; 16: 330.

65. Keshet R, Szlosarek P, Carracedo A, Erez A. Rewiring urea cycle metabolism in cancer to support anabolism. Nat Rev Cancer 2018; 18: 634-645.
66. Murali R, Balasubramaniam V, Srinivas S, et al. Deregulated metabolic pathways in ovarian cancer: cause and consequence. Metabolites 2023; 13: 560.
67. Silberman A, Goldman O, Boukobza Assayag O, et al. Acid-induced downregulation of ASS1 contributes to the maintenance of intracellular pH in cancer. Cancer Res 2019; 79: 518-533.
68. Cheon DJ, Walts AE, Beach JA, et al. Differential expression of argininosuccinate synthetase in serous and non-serous ovarian carcinomas. J Pathol Clin Res. 2015; 1: 41-53.
69. Pénisson-Besnier I, Allamand V, Beurrier P, et al. Compound heterozygous mutations of the TNXB gene cause primary myopathy. Neuromusc Dis 2013; 23: 664-669.
70. Hsia HC, Schwarzbauer JE. Meet the tenascins: multifunctional and mysterious. J Biol Chem 2005; 280: 26641-26644.
71. Liot S, Aubert A, Hervieu V, et al. Loss of tenascin-X expression during tumor progression: a new pan-cancer marker. Matrix Biol Plus 2020; 6-7: 100021.
72. Yuan Y, Nymoen DA, Stavnes HT, et al. Tenascin-X is a novel diagnostic marker of malignant mesothelioma. Am J Surg Pathol 2009; 33: 1673-1682.
73. Nakayama K, Seike M, Noro R, et al. Tenascin XB is a novel diagnostic marker for malignant mesothelioma. Anticancer Res 2019; 39: 627-633.
74. Marcišauskas S, Ulfenborg B, Kristjansdottir B, Waldemarson S, Sundfeldt K. Univariate and classification analysis reveals potential diagnostic biomarkers for early stage ovarian cancer Type 1 and Type 2. J Proteomic 2019; 196: 57-68.
75. Krasny L, Huang PH. Data-independent acquisition mass spectrometry (DIA-MS) for proteomic applications in oncology. Mol Omics 2021; 17: 29-42.
76. Ludwig C, Gillet L, Rosenberger G, Amon S, Collins BC, Aebersold R. Data-independent acquisition-based SWATH-MS for quantitative proteomics: a tutorial. Mol Syst Biol 2018; 14: e8126-e.
77. Yu SH, Kyriakidou P, Cox J. Isobaric matching between runs and novel PSM-level normalization in MaxQuant strongly improve reporter ion-based quantification. J Proteome Res 2020; 19: 3945-3954.

Address for correspondence

Professor Semir Vranic
College of Medicine
Qatar University
Doha, Qatar
e-mail: semir.vranic@gmail.com

Submitted: 03.12.2024
Accepted: 18.01.2025